Development 133, 569-578 doi:10.1242/dev.02220

GLI3-dependent transcriptional repression of *Gli1*, *Gli2* and kidney patterning genes disrupts renal morphogenesis

Ming Chang Hu[1,2], Rong Mo[1], Sita Bhella[1], Christopher W. Wilson[3], Pao-Tien Chuang[3], Chi-chung Hui[1,4] and Norman D. Rosenblum[1,2,5,6,7,*]

Truncating mutations in *Gli3*, an intracellular effector in the SHH-SMO-GLI signaling pathway, cause renal aplasia/dysplasia in humans and mice. Yet, the pathogenic mechanisms are undefined. Here, we report the effect of decreased SHH-SMO signaling on renal morphogenesis, the expression of SHH target genes and GLI binding to *Shh* target genes. *Shh* deficiency or cyclopamine-mediated SMO inhibition disrupted renal organogenesis, decreased expression of GLI1 and GLI2 proteins, but increased expression of GLI3 repressor relative to GLI3 activator. *Shh* deficiency decreased expression of kidney patterning genes (*Pax2* and *Sall1*) and cell cycle regulators (cyclin D1 and MYCN). Elimination of *Gli3* in $Shh^{-/-}$ mice rescued kidney malformation and restored expression of *Pax2*, *Sall1*, cyclin D1, MYCN, *Gli1* and *Gli2*. To define mechanisms by which SHH-SMO signaling controls gene expression, we determined the binding of GLI proteins to 5′ flanking regions containing GLI consensus binding sequences in *Shh* target genes using chromatin immunoprecipitation. In normal embryonic kidney tissue, GLI1 and/or GLI2 were bound to each target gene. By contrast, treatment of embryonic kidney explants with cyclopamine decreased GLI1 and/or GLI2 binding, and induced binding of GLI3. However, cyclopamine failed to decrease *Gli1* and *Gli2* expression and branching morphogenesis in *Gli3*-deficient embryonic kidney tissue. Together, these results demonstrate that SHH-SMO signaling controls renal morphogenesis via transcriptional control of *Gli*, renal patterning and cell cycle regulator genes in a manner that is opposed by GLI3.

KEY WORDS: Kidney development, Sonic Hedgehog, GLI3

INTRODUCTION

Regulation of GLI3 repressor formation via cleavage of GLI3 is crucial during mammalian morphogenesis. *Gli3* mutations that generate a putative truncated protein similar in size to GLI3 repressor are found in humans with Pallister-Hall syndrome (PHS) and malformations including polydactyly, imperforate anus, hypothalamic harmartoma and renal dysplasia/aplasia (Kang et al., 1997). Moreover, mice homozygous for a targeted mutation that generates a 699 amino acid N-terminal GLI3 protein exhibit numerous malformations, including renal aplasia/dysplasia as observed in PHS (Bose et al., 2002). The molecular mechanisms that control these deleterious GLI3-dependent effects are unknown.

GLI3 is an intracellular transcriptional effector in the sonic hedgehog (SHH) signaling pathway. Among the members of the hedgehog (HH) family of secreted proteins, SHH controls cell fate, determination, proliferation and tissue patterning during embryogenesis (reviewed by Ingham and McMahon, 2001). In *Drosophila*, Hh signaling is mediated, at the transcriptional level, by a single zinc-finger protein, Cubitus interruptus (*Ci*) (Methot and Basler, 2001). In the absence of a Hh signal, *Ci* is processed by proteolysis into an N-terminal fragment that includes the zinc finger region and acts to repress gene transcription (Aza-Blanc et al., 1997). In vertebrates, three *Ci* homologs, GLI1, GLI2 and GLI3, mediate Hh signals by controlling gene expression. GLI1 and GLI2 exist as full length proteins in cultured mammalian cells (Dai et al., 1999) and act primarily as transcriptional activators during murine embryogenesis (Bai et al., 2002; Park et al., 2000). Absence of a SHH signal provokes processing of GLI3 into a shortened form that can act as a transcriptional repressor in cultured cells and limb explant cultures (Litingtung et al., 2002; Wang et al., 2000). Genetic analyses in mice demonstrate that the predominant activity of GLI3 is to repress expression of *Shh* dependent genes (Bai et al., 2002; Park et al., 2000). Integration of opposite GLI activities appears to be critical. Genetic inactivation of *Gli3* can rescue *Shh* mutant phenotypes in embryonic tissues including the neural tube (Litingtung and Chiang, 2000), limb (Litingtung et al., 2002), face and forebrain (Rallu et al., 2002), and skin (Mill et al., 2005) suggesting a dynamic interplay between GLI signals during tissue formation. The molecular mechanisms that control such interactions are largely undefined.

The mammalian kidney is a model with which to study embryonic epithelial-mesenchymal interactions and growth factor signaling. In the kidney, interactions between the ureteric bud, an epithelial structure, and the metanephric mesenchyme, a mesenchymal tissue, instigate growth and branching of the ureteric bud, a process known as renal branching morphogenesis, and conversion of the metanephric mesenchyme to those epithelial elements that exist proximal to the ureteric bud branches and their daughter collecting ducts. Growth factors secreted by the ureteric bud and metanephric mesenchymal cells act in a autocrine and paracrine manner to control cellular events including cell proliferation and to control the expression of genes such as *Pax2*, *Sall1* and *Mycn*, each of which performs crucial functions (reviewed by Bouchard, 2004). The presence of renal hypoplasia/dysplasia in mice deficient in *Shh* in the ureteric bud lineage (Yu et al., 2002) and in mice expressing a truncated form of GLI3 (Bose et al., 2002) demonstrates a crucial

[1]Program in Developmental Biology, Hospital for Sick Children, University of Toronto, Toronto, Canada. [2]Division of Nephrology, The Hospital for Sick Children, University of Toronto, Toronto, Canada. [3]Cardiovascular Research Institute, University of California, San Francisco, CA, USA. [4]Department of Medical and Molecular Genetics, University of Toronto, Toronto, Canada. [5]Department of Paediatrics, University of Toronto, Toronto, Canada. [6]Department of Physiology, University of Toronto, Toronto, Canada. [7]Department of Laboratory Medicine and Pathobiology, University of Toronto, Toronto, Canada.

*Author for correspondence (e-mail: norman.rosenblum@sickkids.ca)

Accepted 24 November 2005

role for SHH-GLI signaling during mammalian renal development. However, the molecular mechanisms by which GLI3 controls renal embryogenesis are unknown.

To identify mechanisms by which SHH-GLI signaling controls renal organogenesis, we generated models of deficient SHH or SMO signaling in mutant mice and cultured embryonic kidneys. Homozygous inactivation of *Shh* or treatment of pregnant wild-type mice with cyclopamine, a steroidal alkaloid that blocks SMO activity (Chen et al., 2002), caused renal aplasia or dysplasia. Although these states lowered the expression of both GLI1 and GLI2 protein, the relative expression of a shortened form of GLI3 was increased relative to full-length GLI3 protein. Homozygous inactivation of *Gli3* in a *Shh*-deficient background normalized the renal phenotype and rescued kidney expression of *Pax2*, *Sall1*, cyclin D1 and MYCN, as well as GLI1 and GLI2. We defined mechanisms by which GLI3 controls expression or these SHH targets using chromatin immunoprecipitation. In normal kidney tissue, GLI1 and/or GLI2 bound a GLI-binding consensus region within each target gene 5′ flanking region. By contrast, in cyclopamine-treated malformed cultured kidneys, we observed decreased associations with GLI1/GLI2 and de novo associations with GLI3. Genetic inactivation of *Gli3* alone blocked inhibition of GLI1 and GLI2 expression, and renal branching morphogenesis by cyclopamine. We propose a model in which SHH-SMO signaling controls generation of a GLI3 repressor, which, in turn, controls *Gli1* and *Gli2* as well as non-*Gli* target genes crucial to embryonic kidney development.

MATERIALS AND METHODS

Generation of mice

$Shh^{+/-}$ (Chiang et al., 1996), $Gli2^{+/-}$ (Mo et al., 1997) and $Gli3^{+/-}$ (Schimmang et al., 1992) CD1/129 mice were housed in the Animal Facility of The Hospital for Sick Children (Toronto, Canada) and genotyped by PCR as described previously (Chiang et al., 1996; Mo et al., 1997). Animal experiments were approved by the ethics committee at The Hospital for Sick Children.

Antibodies and specialized reagents

Antibodies and reagents were as follows: GLI1 (Abcam, Cambridge, MA); cyclin D1 (BD PharMingen, San Diego, CA); GLI3, MYCN, MYC, cyclin D2 (Santa Cruz Biotechnology, Santa Cruz CA); cyclopamine (Toronto Research Chemicals, Toronto, ON); and SHH-N (B & D Systems, Minneapolis, MN). A partial mouse *Gli2* cDNA corresponding to amino acids 327-442 was cloned into the pGEX1 vector (Amersham). Fusion protein was expressed in *E. coli* (BL21) and purified on glutathione sepharose (Amersham) according to the manufacturer's instructions. Antibodies were affinity purified using a column of Affi-gel 10 beads (BioRad) conjugated with His-tagged GLI2 antigen. Cyclopamine was dissolved in 100% ethanol for culture of kidney explants and dissolved in 45% 2-hydroxypropyl-beta-cyclodextrin (HBC, Sigma-Aldrich, St Louis, MO) in PBS for intraperitoneal injection. Shh-N was dissolved in 1% FBS in PBS.

Immunohistochemistry and immunoblotting

Immunohistochemistry in paraffin wax-embedded sections (4 μm) of kidney tissue was performed (Hu et al., 2003) with the following antibodies: mouse anti-GLI1 (1:10), rabbit anti-GLI2 (1:700) and rabbit anti-GLI3 (1:50). Biotinylated secondary antibodies were used in a biotin-avidin complex assay (Vector laboratories, Burlingame, CA). Immunoblotting of proteins transferred to nylon membrane was performed using the following antibodies, anti-GLI1 (1:3300 dilution), anti-GLI2 (1: 250 dilution), anti-GLI3 (1:250 dilution, Santa Cruz Biotech), anti-MYC (1:250 dilution), anti-MYCN (1:250 dilution), anti-cyclin D1 (1:250 dilution), anti-cyclin D2 (1:250 dilution) and anti-β-actin (1:3000 dilution, Sigma, St Louis, MO). Secondary anti-mouse IgG and anti-rabbit IgG conjugated HRP (Amersham Pharmacia Biotech, Piscataway, NJ) were used at a 1:3000 and 1:5000 dilution, respectively. Chemiluminescence was performed using commercially available reagents (ECL kit; Amersham Pharmacia Biotech, Piscataway, NJ).

Embryonic kidney organ culture

Kidneys were surgically dissected from mouse embryos and cultured on 0.45 mm polyethylene terephthalate membranes (Corning) in multiwell plates in the presence of Richter's modified Dulbecco's modified Eagle's medium-Ham's F-12 nutrient mixture (DMEM-F12) containing 50 μg/ml transferrin (Sigma) (Pichel et al., 1996). Ureteric bud-derived structures were identified in whole-mount kidney specimens with fluorescein isothiocyanate (FITC)-conjugated DBA (20 μg/ml; Vector Labs, Burlington, ON) (Piscione et al., 1997). A ureteric bud branch point was defined as the intersection between two connected branches.

Effect of cyclopamine on kidney development

Pregnant wild-type or $Gli3^{+/-}$ mice were injected via the peritoneum at E 9.5 with cyclopamine (6 mg/kg body weight) once per day for 4 consecutive days. Embryos were then isolated surgically and fixed in 4% paraformaldehyde-PBS. Alternatively, for treatment of cultured embryonic kidney explants, cyclopamine was added to culture medium at a final concentration of 10 μM. Shh-N was dissolved in 1% FBS and added to culture medium at final concentration of 1.0 μg/ml for 4 days.

In situ mRNA hybridization

In situ hybridization was performed in paraffin wax-embedded tissue sections as described (Mo et al., 1997) using probes encoding *Pax2* [kindly provided by Dr Peter Gruss (Stoykova and Gruss, 1994)] and *Sall1* [kindly provided by Dr Ryuichi Nishinakamura (Nishinakamura et al., 2001)]. For whole-mount in situ hybridization, embryos were fixed in 4% paraformaldehyde at 4°C and processed according to published methods (Conlon and Herrmann, 1993).

In situ cell proliferation assay

Cell proliferation in kidneys was assayed by incorporation of 5-bromo-2′-deoxyuridine (BrdU, Roche Molecular Biochemicals, Mannheim, Germany). Pregnant female mice received an intraperitoneal injection of BrdU (100 μg/g body weight) 4 hours prior to scarifying these mice. Identification of BrdU-positive cells was performed by immunostaining as described previously (Cano-Gauci et al., 1999).

Chromatin immunoprecipitation

Chromatin immunoprecipitation was carried out using published methods (Hu and Rosenblum, 2005). GLI consensus binding sites were identified as TGGGTGGTC or GACCACCCA (Lai et al., 2004). Oligodeoxynucleotide primers were designed to encompass these binding sites as follows. Mouse cyclin D1 promoter (GenBank Accession Number AF212040): forward, 5′-AATTCTAAAGGTGGGGGAACA-3′, reverse 5′-GAGACACGATA-GGCTCCTTCC-3′ (148 bp PCR product). Mouse *Mycn* promoter (GenBank Accession Number X06993): forward 5′-TAATATCCCCC-GAGCTTCAA-3′, reverse 5′-AGCTTCGCAAGTACCGCTTC-3′ (254 bp PCR product at annealing temperature 56°C for 30 seconds). Mouse *Sall1* promoter (GenBank Accession Number AC147558): forward 5′-AGG-CGGTGCCTAGGGTCT, reverse 5′-CTGAAGTTTTCGGGAGAAGC-3′ (299 bp PCR product at annealing temperature 54°C for 45 seconds). Mouse *Pax2* promoter (GenBank Accession Number MMU13975): forward 5′-GGGCTTTGCAGCTTTTAGAG-3′, reverse 5′-TTGGCAGAGAA-GTAGCAATCC-3′ (256 bp PCR product at annealing temperature 54°C for 45 seconds), Mouse *Gli1* promoter (ENSEMBL gene ID ENSMUSG00000025407): forward 5′-AGCTTCAGTGCCACCCCAC-3′, reverse 5′-TCGGTCCGAAGGAAGGATATA-3′ (197 bp PCR product at annealing temperature 55°C for 40 seconds). Mouse *Gli2* promoter (ENSEMBL gene ID ENSMUSG00000051835): forward 5′-GTGC-TGAGGCTCCTGACAAT-3′ and reverse 5′-CAGCAGAGCAAGGTG-AACAG-3′ (124 bp PCR product at annealing temperature 55°C for 40 seconds).

Reverse transcriptase-PCR

Total RNA from frozen tissue samples was extracted using the RNeasy Mini kit (Qiagen, Mississauga, ON, Canada) according to the manufacture's protocol. First-strand cDNA was generated from 2 μg total RNA using random hexamers (SuperScript First Strand Synthesis System, Invitrogen). The following primers were used. *Gli1*: forward 5′-ATCACCTGTTGGG-

GATGCTGGAT-3′, reverse 5′-GGCGTGAATAGGACTTCCGACAG-3′ (317 bp product at annealing temperature 56°C for 45 seconds). *Gli2*: forward 5′-GTTCCAAGGCCTACTCTCGCCTG-3′, reverse 5′-CTTGAGCAGTGGAGCACGGACAT-3′ (304 bp product at annealing temperature 56°C for 45 seconds). *Gli3*: forward 5′-AGCAACCAGGAGCCTGAAGTCAT-3′, reverse 5′-GTCTTGAGTAGGCTTTTGTGCAA-3′ (270 bp product at annealing temperature 56°C for 40 seconds). β-actin: forward 5′-TGTTACCAACTGGGACGACA-3′, reverse 5′-CTCTCAGCTGTGGTGGTGAA-3′ (393 bp product). PCR was performed using HotStarTag. The RT-PCR amplified products were separated by agarose gel electrophoresis and stained with ethidium bromide.

Data analysis

Mean differences between groups were analyzed using Student's *t*-test (two-tailed) or by ANOVA using Stat-View statistical analysis program (version 4.01; Abacus Concepts, Berkeley, CA) for more than two groups. Statistical significance was taken at a value of $P<0.05$.

RESULTS

Disruption of kidney development in SHH deficient and cyclopamine treated mice

We determined the requirement for SHH signaling during murine kidney development by analyzing the renal phenotype in SHH-deficient mice and in mice or kidney explants treated with cyclopamine. Analysis of 20 $Shh^{-/-}$ E14.5 embryos revealed bilateral renal aplasia in 50% (Fig. 1C). The remaining 50% exhibited a single ectopic kidney located in the pelvis (Fig. 1D). These ectopic kidneys demonstrated histological features of renal dysplasia including disorganization of structures within the renal parenchyma and cystic renal tubules (Piscione and Rosenblum, 1999) (Fig. 1E). Using a complementary strategy, we used cyclopamine to block SMO function and investigate the function of the SHH-SMO signaling during renal morphogenesis. An intraperitoneal injection of 6 mg/kg cyclopamine daily for 4 consecutive days starting at E9.5 exerted a major deleterious effect on kidney development (Fig. 1H,I). Compared with embryos treated with drug vehicle alone (Fig. 1F,G), the kidneys in cyclopamine treated embryos demonstrated primordial branching of the ureteric bud and a paucity of metanephric-derived epithelial structures. To determine SMO functions after the onset of mesenchymal-epithelial interactions, kidneys were harvested at E11.5 and cultured in the presence of cyclopamine for 4 consecutive days. Qualitative analysis demonstrated marked inhibition of ureteric bud branching identified by Dolichos Biflorus Agglutinin (compare Fig. 1K with 1J). Quantitation of this effect, performed by counting branch point number, showed that cyclopamine inhibited formation of ureteric bud branch points by 40% (branch point number – drug vehicle

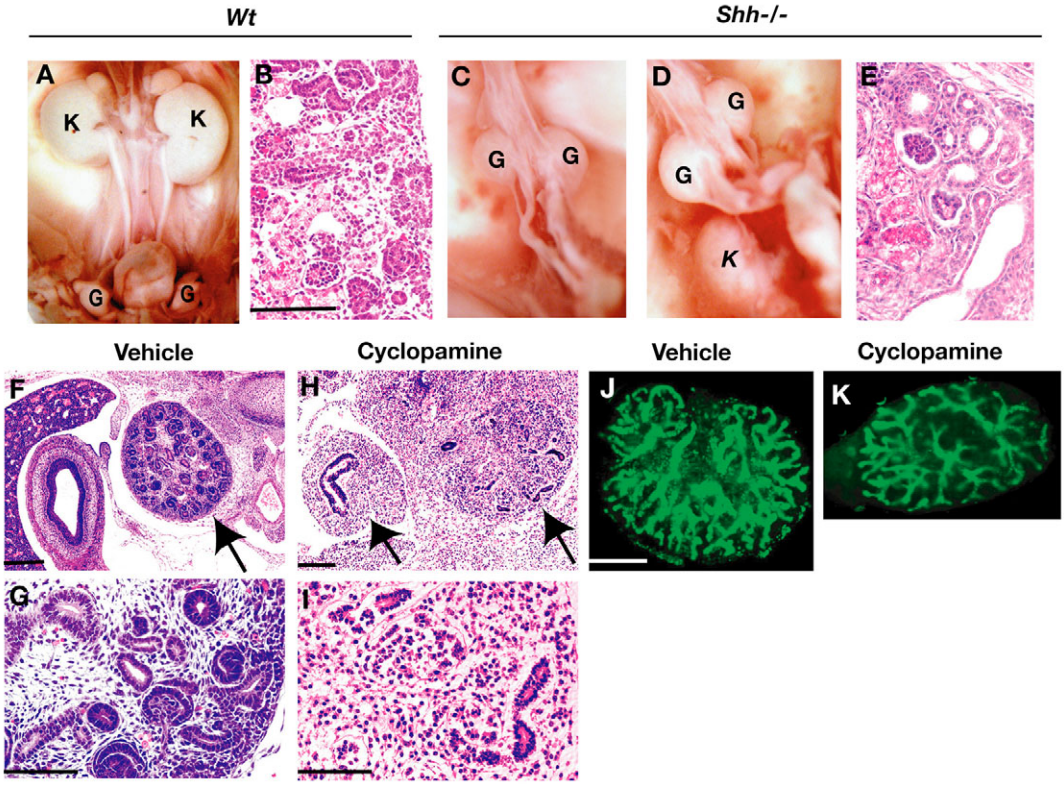

Fig. 1. Deficient SHH-SMO signaling disrupts kidney development. (**A**,**C**,**D**) Gross anatomical features of kidney development in wild-type and $Shh^{-/-}$ mice at E18.5. In contrast to wild-type mice (A), $Shh^{-/-}$ mice exhibited either absence of both kidneys (C) or the presence of a single ectopic kidney located in the pelvis (D). (**B**,**E**) Renal histological phenotype in E18.5 mice. In contrast to the organized appearance of glomeruli and tubules in the renal cortex of wild-type mice (B), the single kidney formed in ~50% of $Shh^{-/-}$ mice (E) was characterized by a paucity of glomeruli and the presence of dilated tubules. Scale bar: 100 μm. (**F-I**) Effect of cyclopamine on renal development. Treatment of mice with cyclopamine starting at E9.5 for four consecutive days blocked renal development. In contrast to kidneys from mice treated with drug vehicle alone (F,G), kidneys in cyclopamine-treated mice (H,I) demonstrated a marked decrease in ureteric bud branches and epithelial metanephric derivatives. Scale bar: 100 μm. (**J**,**K**) Ureteric bud branching in embryonic kidneys isolated at E11.5 from wild-type mice. Kidneys from the same mouse were cultured as pairs in the presence of drug vehicle (J, 100% ethanol in culture medium) or cyclopamine (K) for 4 days. Ureteric bud branches were identified with Dolichos Biflorus Agglutinin. In contrast to vehicle, cyclopamine decreased the number of ureteric bud branches formed. Scale bar: 100 μm. G, gonad; K, kidney.

versus cyclopamine: 61.6±2.4 versus 37.6±1.6; $P<0.0001$. $n=5$ kidneys/group). Analysis of histological sections generated from these kidneys revealed a paucity of metanephric-derived epithelial elements (see Fig. S1 in the supplementary material). Taken together, these results in two complementary models of disrupted SHH-SMO signaling demonstrate a crucial role for SHH-SMO signaling during induction of the metanephric blastema by the ureteric bud and during branching morphogenesis and nephrogenesis.

SHH and SMO control GLI1 and GLI2 expression and formation of GLI3 repressor

In mammals, GLI1, GLI2 and GLI3 are the intracellular effectors of SHH-SMO signaling. Yet the regulation of GLI protein expression in response to SHH is not well understood. We used antibodies specific for distinct GLI proteins to investigate the effects of SHH deficiency and SMO inactivity on GLI expression. The specificity of anti-GLI antibodies was demonstrated by lack of detection of GLI2 and GLI3 in kidneys isolated from *Gli2*$^{-/-}$ (Fig. 2F) and *Gli3*$^{-/-}$ (Fig. 2K) mice, respectively. Expression of GLI1, GLI2 and GLI3 was detected in both the metanephric-derived epithelium and ureteric bud of kidneys isolated from E14.5 wild-type mice (Fig. 2A,E,I). By contrast, homozygous inactivation of *Shh* but not *Gli3* decreased GLI1 and GLI2 protein expression to undetectable levels in dysplastic kidneys (Fig. 2C,D,G,H). GLI3 expression was not affected by SHH deficiency (Fig. 2L).

Analysis of GLI protein expression in kidney tissue lysates confirmed the decrease in GLI1 and GLI2 proteins observed by immunohistochemistry (Fig. 2M). Western analysis provided additional insight into the expression of GLI3 demonstrating a marked decrease in the full-length activator form of GLI3 (190 kDa) with preserved expression of the short repressor form of GLI3 (89 kDa). This resulted in a marked decrease in the ratio of GLI3 activator to GLI3 repressor in tissue isolated from *Shh*$^{-/-}$ mice (GLI3

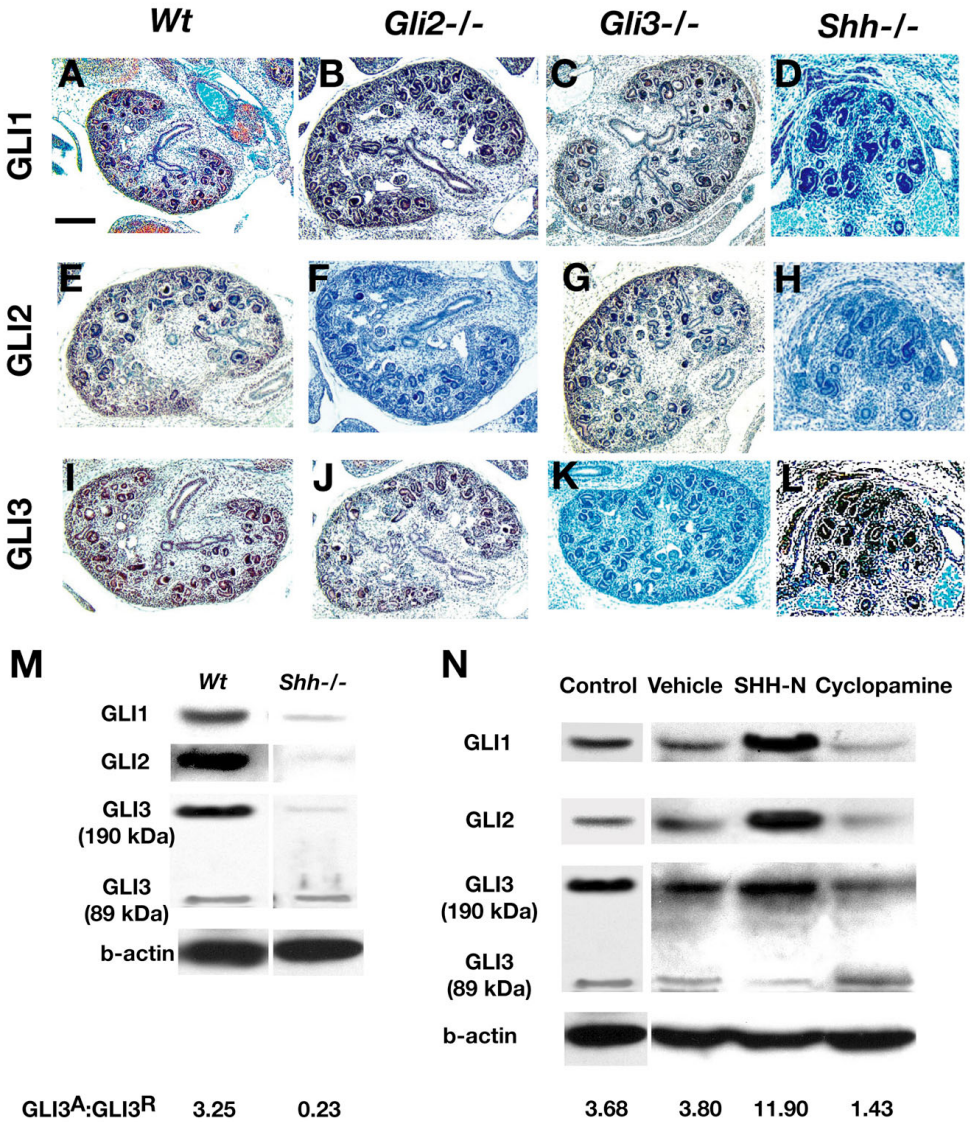

Fig. 2. Effects of *Shh* deficiency or SMO inhibition on GLI protein expression.
(**A**-**L**) Immunohistochemistry of 4 μm tissue sections generated from E14.5 kidney tissue using specific anti-GLI antibodies. The substrate reaction generated a red color. Tissue was counterstained with Hematoxylin (blue). In tissue generated from wild-type mice (A,E,I), GLI1, GLI2 and GLI3 were each detected in metanephric-derived epithelial structures and ureteric bud branches. *Shh* deficiency decreased GLI1 and GLI2 expression compared with wild type (D,H versus A,E). By contrast, total GLI3 expression in kidney was not decreased in *Shh*$^{-/-}$ mice (L). Antibody specificity was demonstrated by lack of staining in corresponding *Gli*-deficient mice (B,C,F,G,J,K). Scale bar: 100 μm. (**M**) Western analysis of E14.5 kidney tissue lysates generated from wild-type and *Shh*$^{-/-}$ mice. *Shh* deficiency decreased GLI1 and GLI2. Although GLI3 activator (190 kDa) was decreased, GLI3 repressor (89 kDa) was unaffected compared with wild type. The ratio of GLI3 activator to GLI3 repressor in renal tissue was markedly decreased from 3.25 in wild type to 0.23 in *Shh*$^{-/-}$ mice. (**N**) Western analysis of tissue lysates generated from cultured embryonic kidneys isolated from E11.5 wild-type mice and treated for 4 days with culture medium alone or with culture medium supplemented with drug vehicle (100% ethanol), SHH-N or cyclopamine. In the presence of culture medium, embryonic kidneys expressed GLI1, GLI2 and GLI3 activator (190 kDa) in excess of GLI3 repressor (89 kDa) (GLI3 activator: GLI3 repressor=3.68). Treatment with SHN-N increased GLI1, GLI2 and the relative expression of GLI3 activator versus GLI3 repressor (GLI3 activator:GLI3 repressor=11.9). Treatment with drug vehicle had no significant effect on GLI protein expression. By contrast, cyclopamine decreased GLI1 and GLI2 and the relative expression of GLI3 activator versus GLI3 repressor (GLI3 activator:GLI3 repressor=1.43).

activator:GLI3 repressor: wild type versus *Shh*$^{-/-}$, 3.25 versus 0.23). We observed similar changes in GLI protein expression in cyclopamine-treated wild-type embryonic kidney explants (Fig. 2N). First, cyclopamine decreased GLI1 and GLI2 protein expression. Second, cyclopamine increased formation of GLI3 repressor and decreased levels of GLI3 activator, albeit to a more modest degree than that observed in *Shh*$^{-/-}$ mice. Third, cyclopamine decreased the ratio of GLI3 activator to GLI3 repressor (GLI3 activator:GLI3 repressor – culture medium alone versus drug vehicle versus SHH-N versus cyclopamine, 3.68 versus 3.8 versus 11.9 versus 1.43, respectively). Together, these data demonstrate that SHH deficiency or SMO inhibition decreases GLI1 and GLI2 and increases the relative expression of GLI3 repressor.

Gli3 inactivation rescues kidney dysplasia and SHH target gene expression

To investigate the impact of increased GLI3 repressor on kidney development, we analyzed *Shh*$^{-/-}$;*Gli3*$^{-/-}$ mice at different developmental stages. During murine kidney development, *Pax2*, a member of the paired box family of transcription factors, is expressed in the Wolffian Duct, ureteric bud and induced metanephric blastema and is required for metanephric development (Dressler et al., 1990; Torres et al., 1995) (Fig. 3A). Thus, we used *Pax2* mRNA expression as a marker of early inductive events (Fig. 3A). Consistent with the finding of renal aplasia in 50% *Shh*$^{-/-}$ mice, *Pax2* mRNA expression was barely detectable in ~50% of *Shh*$^{-/-}$ mice (Fig. 3B). In the remaining *Shh*$^{-/-}$ embryos, *Pax2* mRNA was detected in the metanephros (Fig. 3C). Although loss of *Gli3* function alone had no effect on *Pax2* mRNA expression (Fig. 3D), it restored *Pax2* mRNA expression in all *Shh*$^{-/-}$;*Gli3*$^{-/-}$ mice (Fig. 3E). Next, we investigated the role of *Gli3* at a later developmental stage when branching morphogenesis and metanephric epithelialization are established. By E13.5, *Pax2* is normally expressed in both the induced metanephric mesenchyme and ureteric bud branches (Fig. 3K). In addition, *Sall1* expression is localized to the metanephric mesenchyme (Fig. 3P). Both *Pax2* and *Sall1* are required for metanephrogenesis at this stage (Nishinakamura et al., 2001; Rothenpieler and Dressler, 1993). Using *Pax2* and *Sall1* as markers of ureteric bud and metanephric development, we observed rescue of kidney number, histology and *Pax2* and *Sall1* expression in *Shh*$^{-/-}$;*Gli3*$^{-/-}$ mice (Fig. 3J,O,T) compared with *Shh*$^{-/-}$ mice (Fig. 3G,L,Q). Interestingly, deficiency of neither *Gli2* nor *Gli3* interfered with expression of *Pax2* (Fig. 3M,R) and *Sall1* (Fig. 3N,S). Taken together, these data demonstrate that the deleterious effect of SHH deficiency on kidney development is dependent on GLI3.

Growth factor-dependent control of cell proliferation is tightly regulated during kidney development. Dysregulation of cell proliferation results in renal dysplasia (Michael and Davies, 2004). We determined the impact of altered SHH signaling on cell proliferation by measuring incorporation of 5-bromodeoxyuridine (BrdU), a surrogate marker of cell proliferation, in embryonic kidneys (Fig. 4). Qualitative analysis of kidney sections stained with anti-BrdU antibody (Fig. 4A-D) revealed incorporation of BrdU in epithelial and mesenchymal derivatives located on the outer regions of kidneys isolated from wild-type, *Gli3*$^{-/-}$ and *Shh*$^{-/-}$;*Gli3*$^{-/-}$ kidneys. By contrast, BrdU incorporation was markedly diminished in *Shh*$^{-/-}$ kidneys. Quantitation of the number of BrdU-positive cells in ureteric bud branches, identified by Dolichos Biflorus Agglutinin (Grisaru et al., 2001), and in mesenchymal cells demonstrated an approximate twofold and fourfold diminution of cell proliferation in the ureteric bud and metanephric mesenchyme, respectively, in kidney tissue from *Shh*$^{-/-}$ mice compared with wild type (Fig. 4E). By contrast, in kidneys isolated from *Shh*$^{-/-}$;*Gli3*$^{-/-}$ mice, cell proliferation in both these tissue compartments was rescued to levels

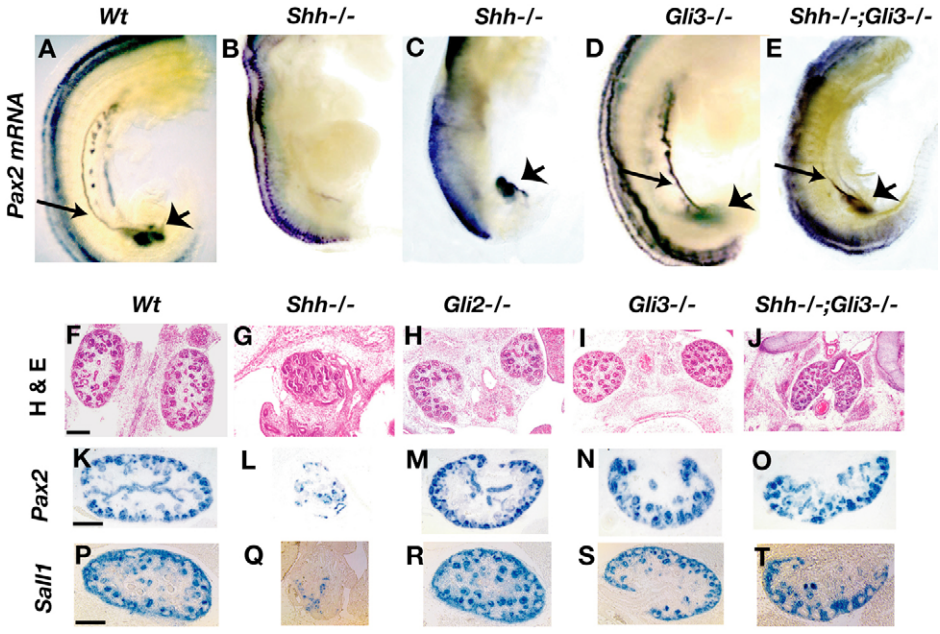

Fig. 3. *Shh* and *Gli3* interact to control *Pax2* and *Sall1* expression during kidney development. (**A-E**) *Pax2* mRNA expression in E11.5 mouse embryos. *Pax2* mRNA was identified by whole-mount in situ hybridization using digoxigenin-labeled probes. In wild-type and *Gli3*$^{-/-}$ embryos, *Pax2* mRNA is expressed in the Wolffian duct (long arrow) and metanephros (short arrow). *Pax2* mRNA was barely detectable in the Wolffian duct in ~50% of *Shh*$^{-/-}$ embryos (compare B with A). *Pax2* mRNA was rescued to wild-type levels in all *Shh*$^{-/-}$;*Gli3*$^{-/-}$ embryos examined. (**F-J**) Kidney histology in E14.5 embryos. Tissue sections (4 μm) were stained with Hematoxylin. Wild-type (F), *Gli2*$^{-/-}$ (H) and *Gli3*$^{-/-}$ (I) mice exhibit two normally positioned kidneys. A single, ectopic, dysplastic kidney was observed in *Shh* deficient mice (G). By contrast, kidney number and histology was rescued in *Shh*$^{-/-}$;*Gli3*$^{-/-}$ mice (J). Scale bar: 200 μm. (**K-O**) *Pax2* mRNA expression in E14.5 mouse kidneys. *Pax2* mRNA was detected using a digoxigenin-labeled probe and in situ hybridization in 4 μm tissue sections. In wild-type (K), *Gli2*$^{-/-}$ (M) and *Gli3*$^{-/-}$ (N) kidneys, *Pax2* mRNA was expressed in ureteric bud branches and metanephric-derived epithelial structures. In *Shh*$^{-/-}$ mice (L), *Pax2* mRNA expression was markedly diminished but was rescued in *Shh*$^{-/-}$;*Gli3*$^{-/-}$ mice (O). Scale bar: 100 μm. (**P-T**) *Sall1* mRNA expression in E14.5 mouse kidneys. *Sall1* mRNA was detected using a digoxigenin-labeled probe and in situ hybridization in 4 μm tissue sections. In wild-type (P), *Gli2*$^{-/-}$ (R), and *Gli3*$^{-/-}$ (S) kidneys, *Sall1* mRNA was expressed in metanephric-derived epithelial structures. In *Shh*$^{-/-}$ mice (Q), *Sall1* mRNA expression was markedly diminished but was rescued in *Shh*$^{-/-}$;*Gli3*$^{-/-}$ mice (T). Scale bar: 100 μm.

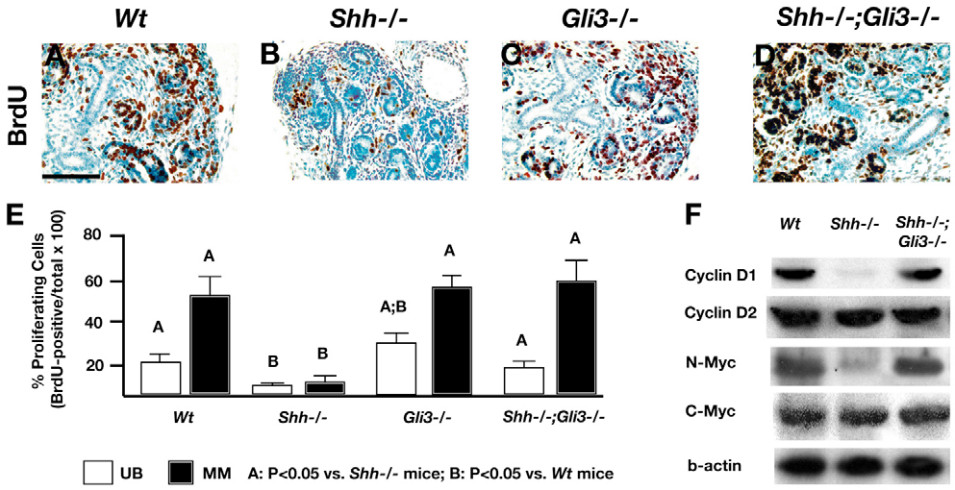

Fig. 4. *Shh* and *Gli3* interact to control cell proliferation and expression of cell cycle regulatory proteins. (**A-D**) In situ analysis of BrdU incorporation at E14.5. Pregnant mice were injected with BrdU and sacrificed 4 hours later. BrdU incorporation was detected by an in situ BrdU incorporation assay. Red-stained nuclei are BrdU positive. Tissues were counterstained with Hematoxylin (blue). In wild-type (A), *Gli3*$^{-/-}$ (C) and *Shh*$^{-/-}$;*Gli3*$^{-/-}$ (D) mice, BrdU incorporation was observed in metanephric mesenchyme cells, mesenchyme-derived epithelial structures and ureteric bud tips. In *Shh*$^{-/-}$ mice (B), BrdU incorporation was markedly decreased. Scale bar: 100 μm. (**E**) Quantitative analysis of BrdU incorporation at E14.5. BrdU incorporation is expressed as a fraction of the total number of cells in the ureteric bud (white bars) and its branches or in the metanephric mesenchyme (black bars). *Shh* deficiency decreased BrdU incorporation in both ureteric bud and mesenchyme-derived epithelial structures significantly compared with wild type. Removal of *Gli3* in *Shh*$^{-/-}$ mice rescued BrdU incorporation to levels not significantly different than those observed in wild type. Removal of *Gli3* increased BrdU incorporation in ureteric bud derived cells to a level greater than that observed in wild type. (**F**) Western analysis of E14.5 kidney tissue lysates. Expression of cyclin D1 and MYCN was markedly decreased in *Shh*$^{-/-}$ compared with wild type and was rescued to wild-type levels in *Shh*$^{-/-}$;*Gli3*$^{-/-}$ mice. By contrast, expression of cyclin D2 and MYC was not affected by *Shh* deficiency.

observed in wild-type tissue. Interestingly, a higher rate of ureteric bud cell proliferation was observed in *Gli3* deficient mice compared with wild type.

In nonrenal tissues, members of the cyclin and MYC families regulate cell proliferation in a SHH-dependent manner (Li et al., 2004; Mill et al., 2005). Thus, we determined the effect of SHH deficiency on the expression of cyclin D1, cyclin D2, MYCN and MYC in the kidney of SHH-deficient mice using specific antibodies and western analysis (Fig. 4F). Although each of these gene products is expressed in the embryonic kidney in wild-type mice, the expression of both cyclin D1 and MYCN was greatly diminished in kidneys isolated from *Shh*$^{-/-}$ mice but was rescued in the kidneys of *Shh*$^{-/-}$;*Gli3*$^{-/-}$ mice. Together, these data demonstrate a crucial role for GLI3 in controlling the response to SHH deficiency at the level of cell proliferation and target gene expression.

Inhibition of SMO changes the association of GLI proteins with GLI-binding consensus regions within SHH target genes

We determined how differential control of GLI1, GLI2 and GLI3 by SHH-SMO signaling controls the expression of SHH target genes in the kidney. First, we identified putative GLI-binding consensus sequences (Ikram et al., 2004; Kinzler and Vogelstein, 1990; Sasaki et al., 1997) in the 5′ flanking regions of *Pax2*, *Sall1*, cyclin D1 and *Mycn* (Fig. 5A). Next, we used chromatin immunoprecipitation to analyze the association of GLI1, GLI2 or GLI3 with regions encompassing these sequences. Our results indicate that GLI1 and/or GLI2, but not GLI3, bind these promoter elements in wild-type kidneys either cultured in vitro (Fig. 5B) or processed immediately after isolation (see Fig. S2 in the supplementary material). Treatment of embryonic kidney explants with cyclopamine induced changes in GLI protein binding with these target promoters (Fig. 5B). Most remarkably, the binding of GLI1 and GLI2 with *Pax2* and *Sall1* was barely detectable. Strikingly, we observed de novo binding of GLI3 with each of these promoters. These results demonstrate that decreased SMO signaling changes induces the de novo association of GLI3 and decreases the association of GLI1 and GLI2 with target promoters.

GLI3 controls decreased GLI1 and GLI2 expression in SHH deficient mice

Our genetic analyses in *Shh*$^{-/-}$ mice demonstrated that *Shh* deficiency decreases GLI1 and GLI2 as well as expression of *Shh* target genes. By contrast, removal of both *Gli3* and *Shh* restored expression of *Shh* target genes. To determine whether Gli3 plays a primary role in orchestrating these events, we investigated whether Gli3 controls Gli1 and Gli2 in *Shh*$^{-/-}$;*Gli3*$^{-/-}$ mice. Analysis of GLI protein expression in kidney tissue lysates demonstrated rescue of GLI1 and GLI2 levels in *Shh*$^{-/-}$;*Gli3*$^{-/-}$ mice to the levels observed in wild-type mice (Fig. 6A). To determine whether GLI3 controls GLI1 and GLI2 expression at a transcriptional level, we examined mRNA in kidney tissue isolated from wild-type and *Shh*$^{-/-}$;*Gli3*$^{-/-}$ mice using reverse transcriptase PCR (Fig. 6B). Although *Gli1* and *Gli2* mRNA levels were decreased in *Shh*$^{-/-}$ mice, the levels of these mRNAs were rescued to wild-type levels in *Shh*$^{-/-}$;*Gli3*$^{-/-}$ mice. These results provided a basis for determining how GLI3 controls *Gli1* and *Gli2* transcription. First, we identified GLI binding sites in the 5′ flanking regions of *Gli1* and *Gli2* (Fig. 6C). Next, we examined the association of GLI proteins with these sites by chromatin immunoprecipitation. Analysis of the regions encoding GLI binding sequences in wild-type kidneys either cultured in vitro (Fig. 6D) or processed immediately after isolation (see Fig. S3 in the supplementary material) demonstrated that GLI2 bound both *Gli1* and *Gli2*. A weaker association was observed between GLI1 and *Gli1* or *Gli2* and between GLI3 and *Gli2*. cyclopamine enhanced binding between GLI3 and the *Gli1* promoter and between GLI3 and the *Gli2* promoter. By contrast, the associations with GLI2 were decreased to almost undetectable levels. Our concurrent finding that cyclopamine decreased mRNAs encoding *Gli1* and *Gli2* and *Pax2* showed that these effects in vitro

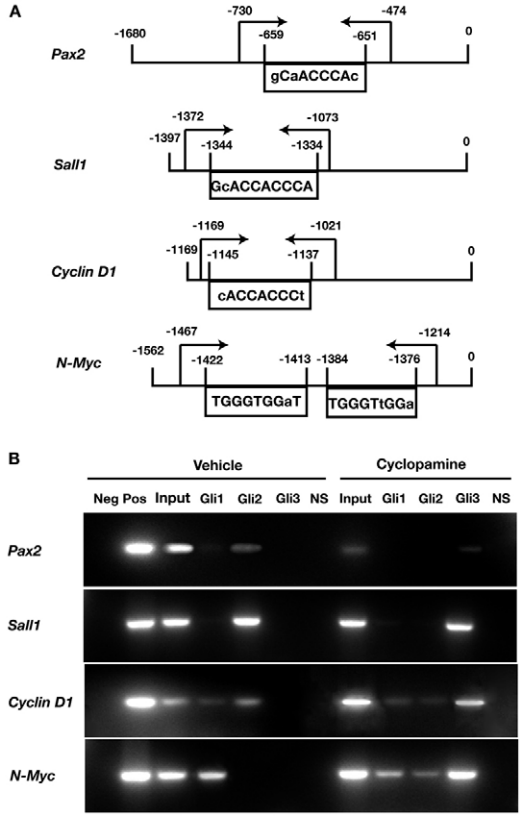

Fig. 5. cyclopamine changes binding of GLI protein species to 5′ flanking regions in *Shh* target genes. (**A**) Identification of GLI consensus binding sequences in the 5′ flanking region of mouse *Pax2*, *Sall1*, cyclin D1 and *Mycn*. Nucleotides represented in upper case are exact matches to those identified previously in GLI consensus binding sequences (see text). Arrows indicate promoter segments amplified by PCR during chromatin immunoprecipitation (see below). (**B**) PCR products identified by agarose electrophoresis after chromatin immunoprecipitation using E11.5 wild-type kidney tissue cultured for 4 days in the presence of drug vehicle or cyclopamine. In vehicle-treated embryonic kidneys, GLI1 and/or GLI2 bound 5′ flanking regions containing GLI consensus binding regions in *Pax2*, *Sall1*, cyclin D1 and *Mycn*. No binding of GLI3 with these regions was detectable. Cyclopamine decreased GLI1 and GLI2 binding most markedly in *Pax2* and *Sall1*, and induced binding of GLI3 to each promoter region. Neg, DNA amplified after immunoprecipitation with non-immune serum; Pos, DNA amplified using genomic DNA and specific primers; Input, DNA amplified from cross-linked DNA before immunoprecipitation.

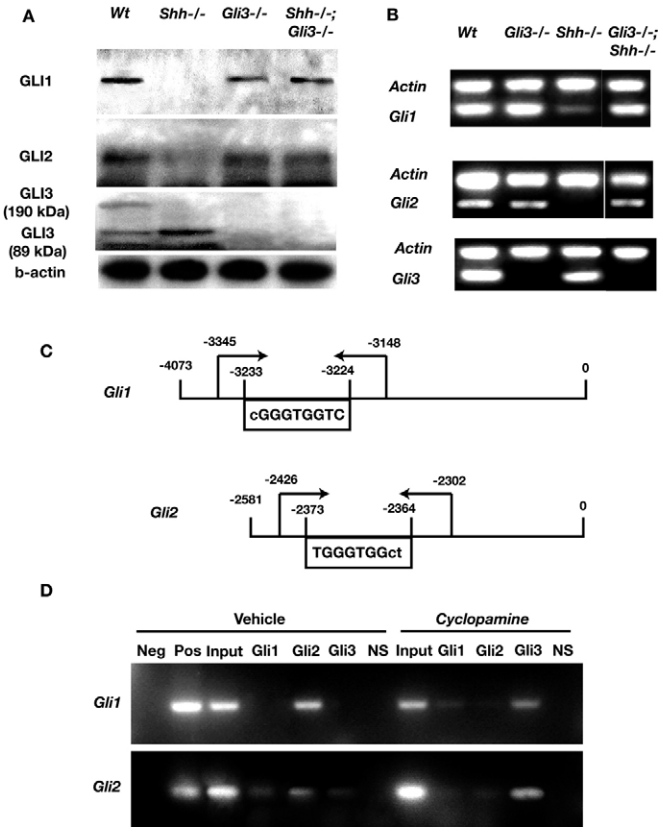

Fig. 6. GLI3 controls GLI1 and GLI2 expression via transcriptional mechanisms. (**A**) Western analysis of E14.5 kidney tissue lysates using specific anti-GLI antibodies. In $Shh^{-/-}$ mice, expression of GLI1 and GLI2 was decreased compared with wild type and $Gli3^{-/-}$. In $Shh^{-/-};Gli3^{-/-}$ mice, GLI1 and GLI2 expression was rescued to wild-type levels. (**B**) Agarose gel electrophoresis of products generated by RT-PCR using RNA isolated from E14.5 embryonic kidney. Expression of *Gli1* and *Gli2* mRNA was decreased in $Shh^{-/-}$ compared with wild type and $Gli3^{-/-}$ and was rescued in $Shh^{-/-};Gli3^{-/-}$ mice. (**C**) Identification of GLI consensus binding sequences in the 5′ flanking region of mouse *Gli1* and *Gli2*. Nucleotides represented in upper case are exact matches to those identified previously in GLI consensus binding sequences (see text). Arrows indicate promoter segments amplified by PCR during chromatin immunoprecipitation (see below). (**D**) PCR products identified by agarose electrophoresis after chromatin immunoprecipitation using E11.5 wild-type kidney tissue cultured for 4 days in the presence of drug vehicle or cyclopamine. In vehicle-treated embryonic kidneys, GLI1 and/or GLI2 bound 5′ flanking regions containing GLI consensus binding regions in *Gli1* and *Gli2*. No binding of GLI3 with this region in *Gli1* was detectable. Cyclopamine decreased GLI1 and GLI2 binding and induced binding of GLI3 to each promoter region. Neg, DNA amplified after immunoprecipitation with non-immune serum; Pos, DNA amplified using genomic DNA and specific primers; Input, DNA amplified from cross-linked DNA before immunoprecipitation.

paralleled our findings in vivo (see Fig. S4 in the supplementary material). Together, these results demonstrate that GLI3 binds to the *Gli1* and *Gli2* promoters when SHH-SMO signaling is inhibited.

To investigate whether Gli3 is primarily involved in controlling *Gli1* and *Gli2* expression, we analyzed their expression in cyclopamine-treated embryonic kidney explants isolated from $Gli3^{-/-}$ mice. Our prior results (Fig. 6) predicted that cyclopamine would fail to decrease GLI1 and GLI2 in GLI3 deficient tissue. In kidneys isolated from wild-type mice, cyclopamine markedly decreased GLI1 and GLI2 (Fig. 7A) and branching morphogenesis (Fig. 7B). By contrast, we observed no effect of cyclopamine on GLI1 and GLI2 or ureteric bud branching in tissue isolated from $Gli3^{-/-}$ mice (Fig. 7A,B). Thus, GLI3 controls GLI1 and GLI2 expression and renal morphogenesis when SMO is inhibited.

DISCUSSION

The experiments reported here demonstrate that decreased SHH-SMO signaling disrupts kidney development and regulates GLI3 expression in a manner distinct from that of GLI1 and GLI2. Expression of the repressor form of GLI3 is increased, while its full-length form and that of GLI2 and GLI3 is decreased. The significance of GLI3 repressor formation was demonstrated by our finding that homozygous GLI3 deficiency in *Shh* deficient mice rescued the dysplastic renal phenotype and the expression of *Pax2*, *Sall1*, cyclin D1 and *Mycn*. Analysis of GLI protein association with GLI consensus binding regions in the 5′ flanking regions of these target genes provides a novel insight into potential mechanisms by which GLI3 controls gene expression. Binding of GLI1 and GLI2 to the *Pax2*, *Sall1*, cyclin D1 and *Mycn* promoters established these genes as direct targets of SHH. De novo GLI3 binding to these same regions in a state of SMO inactivity suggests that GLI3 directly represses these genes. Decreased expression of GLI1 and GLI2 and decreased binding of these proteins to their target genes raised the possibility that GLI3 regulates GLI1 and GLI2 expression. Binding of GLI3 to the *Gli1* and *Gli2* promoters in tissue treated to inhibit SMO supported this hypothesis. Our demonstration that *Gli3* deficiency abrogates the deleterious effects of SMO inhibition on GLI1 and GLI2 expression and normalizes branching morphogenesis provided functional support for our hypothesis. Together, our results indicate that SHH-SMO signaling regulates the formation of GLI3 repressor. In a state of decreased SHH-SMO signaling, GLI3 represses GLI1, GLI2 and genes crucial to renal morphogenesis.

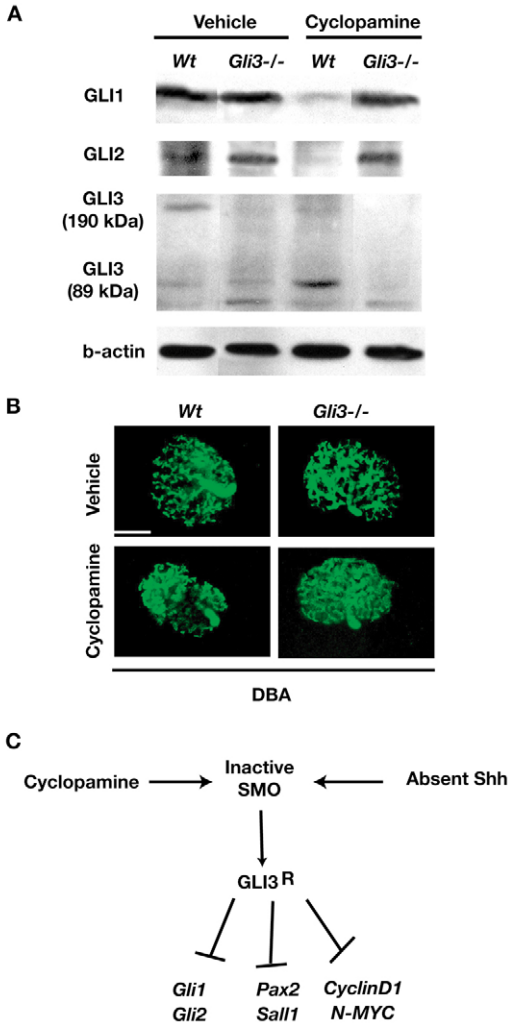

Fig. 7. *Gli3* is required for SMO-dependent control of GLI expression and kidney development. (**A**) Western analysis of kidney tissue lysates using GLI-specific antibodies. Embryonic kidneys were harvested from wild-type or *Gli3*$^{-/-}$ mice at E11.5 and cultured in the presence of drug vehicle or cyclopamine for 4 days. Treatment of kidneys isolated from wild-type mice with cyclopamine markedly decreased GLI1 and GLI2. This inhibitory effect was totally abrogated in *Gli3*-deficient mice. (**B**) Ureteric bud branching in cultured kidney explants. Treatment of kidneys isolated from E11.5 wild-type mice with cyclopamine decreased the number of ureteric bud branches identified by Dolichos Biflorus Agglutinin. This inhibitory effect was abrogated in *Gli3*-deficient mice. (**C**) Model of GLI3 activity in a state of SMO inhibition. Decreased SMO activity generated by SHH deficiency or treatment with cyclopamine increases formation of GLI3 repressor. GLI3 repressor controls expression of *Gli1* and *Gli2* as well as SHH target genes that control renal morphogenesis (*Pax2* and *Sall1*) and cell proliferation (cyclin D1 and *Mycn*).

A requirement for SHH-SMO signaling during kidney development

Our results demonstrate a requirement for SHH-SMO signaling during kidney development. What are the mechanisms that underlie this requirement? One possibility is loss of one or more GLI activator functions. *Gli1*, *Gli2* and *Gli3* have all been shown to function as SHH-SMO-dependent activators in nonrenal tissues in a context-dependent manner (Bai et al., 2004; Buttitta et al., 2003; McDermott et al., 2005). Yet, homozygous deficiency of *Gli1*, Gli2 and *Gli3* does not negatively impact murine kidney development (Bai et al., 2002; Kim et al., 2001; Schimmang et al., 1992). By contrast, mutations that generate expression of a shortened repressor-like form of GLI3 in humans with Pallister-Hall syndrome (Kang et al., 1997) and in genetically engineered mice (Bose et al., 2002) also disrupt kidney development. Our studies provide novel insights into the potential actions of GLI3 repressor showing that when SMO is inhibited, GLI3 controls *Gli1* and *Gli2* expression and associates with the *Gli1* and *Gli2* promoters. These findings suggest that in Pallister-Hall syndrome, GLI3 represses *Gli1* and *Gli2* as well as *Pax2*, *Sall1*, cyclin D1 and *Mycn* via interactions with their respective promoter elements. More generally, our findings provide insight into the observation that genetic inactivation of *Gli3* can rescue Shh mutant phenotypes in nonrenal tissues (Litingtung and Chiang, 2000; Litingtung et al., 2002; Mill et al., 2005; Rallu et al., 2002). Our results suggest that in these different developmental contexts GLI3 repressor directly controls *Gli* transcription and that of *Gli*-dependent target genes.

Kidney patterning genes are direct GLI transcriptional targets

Our results provide new insights into the target genes regulated by SHH and SMO, demonstrating that *Shh* acts upstream of *Pax2* and *Sall1*. Both *Pax2* and *Sall1* perform crucial functions during murine renal organogenesis (Nishinakamura et al., 2001; Rothenpieler and Dressler, 1993). Mutations in *PAX2* are associated with renal coloboma syndrome and renal hypoplasia (Sanyanusin et al., 1995). Homozygous inactivation of *Pax2* in mice results in renal aplasia or severe dysgenesis (Rothenpieler and Dressler, 1993), indicating a requirement for *Pax2* during outgrowth of the ureteric bud and invasion of the metanephric blastema. The observation that *Pax2* controls expression of *Gdnf* (Brophy et al., 2001), which encodes a

secreted growth factor essential for outgrowth and invasion by the ureteric bud (Moore et al., 1996), suggests that *Shh* acts upstream of the GDNF-RET signaling pathway during renal organogenesis. *SALL1* mutations are found in individuals with Townes Brock syndrome and renal aplasia/dysplasia (Kohlhase et al., 1998). During murine kidney development, *Sall1* expression is restricted to the metanephric mesenchyme where it is essential as homozygous inactivation of *Sall1* abrogates outgrowth of the ureteric bud (Nishinakamura et al., 2001). Our results provide novel insight into *Sall1* regulation showing that it is controlled by *Shh*.

Our results using chromatin immunoprecipitation extend our genetic analyses and demonstrate that promoter elements in both *Pax2* and *Sall1* are bound by GLI1, GLI2 and GLI3 to variable degrees and in different combinations, depending, in part, on the state of SHH-SMO signaling.

GLI transcriptional control of target genes is dependent on context

Our results demonstrate that SHH controls cell proliferation and expression of cyclin D1 and MYCN during kidney development as in non-renal embryonic tissues (Long et al., 2001; Mill et al., 2005). Interestingly, while cyclin D2 is regulated by SHH in the developing hair follicle (Mill et al., 2005), cyclin D2 expression is independent of *Shh* expression in the embryonic kidney. The mechanisms by which GLI proteins mediate the actions of SHH to control cell proliferation appear to differ between skin and kidney. In skin, both *Shh* and *Gli2* control cell proliferation (Mill et al., 2005). In kidney, *Gli2* deficiency does not affect cell proliferation (data not shown). In both skin and kidney *Gli3* deficiency rescues decreased cell proliferation observed in $Shh^{-/-}$ mice. However, the degree of rescue is much greater in kidney compared with skin, suggesting that other factors modulate the actions of GLI proteins to control cell proliferation. These factors may include GSK3β and β-catenin (Mill et al., 2005). The relevance of this mode of regulation to kidney development requires further investigation.

A model of gene regulation in states of decreased SHH-SMO activity

The experiments reported here provide a basis for a model that predicts that *Gli3* acts downstream of SMO and upstream of *Gli1* and *Gli2* in the developing kidney and that *Shh* programs kidney morphogenesis by restricting the activity of GLI3. In our model, GLI3 repressor orchestrates the effects of SMO inhibition, thereby disrupting kidney morphogenesis (Fig. 7C). GLI3 repressor acts by inhibiting the transcription of several classes of genes, the actions of which are crucial to kidney development (Fig. 7C). The first is the Gli family, specifically *Gli1* and *Gli2*. The second class of genes includes those crucial to renal patterning. Members of this class include *Pax2* and *Sall1*. The third class of genes is that controlling cell proliferation and includes cyclin D1 and MYCN. Formation of GLI3 repressor is critical to repression of these genes. Our findings provide a basis for investigating molecular mechanisms that control the interplay of GLI1, GLI2 and GLI3 in the regulation of these SHH-SMO target genes.

This work was supported by operating grants awarded by the Canadian Institutes of Health Research (to N.D.R. and C.C.H.). We thank Ya-Jun Li for technical assistance. Work in the Chuang laboratory was supported by an NIH grant (HL67822). N.D.R. is supported by a Canada Research Chair.

Supplementary material

Supplementary material for this article is available at http://dev.biologists.org/cgi/content/full/133/3/569/DC1

References

Aza-Blanc, P., Ramirez-Weber, F. A., Laget, M. P., Schwartz, C. and Kornberg, T. B. (1997). Proteolysis that is inhibited by hedgehog targets Cubitus interruptus protein to the nucleus and converts it to a repressor. *Cell* **89**, 1043-1053.

Bai, C. B., Auerbach, W., Lee, J. S., Stephen, D. and Joyner, A. L. (2002). Gli2, but not Gli1, is required for initial Shh signaling and ectopic activation of the Shh pathway. *Development* **129**, 4753-4761.

Bai, C. B., Stephen, D. and Joyner, A. L. (2004). All mouse ventral spinal cord patterning by hedgehog is Gli dependent and involves an activator function of Gli3. *Dev. Cell* **6**, 103-115.

Bose, J., Grotewold, L. and Ruther, U. (2002). Pallister-Hall syndrome phenotype in mice mutant for Gli3. *Hum. Mol. Genet.* **11**, 1129-1135.

Bouchard, M. (2004). Transcriptional control of kidney development. *Differentiation* **72**, 295-306.

Brophy, P. D., Ostrom, L., Lang, K. M. and Dressler, G. R. (2001). Regulation of ureteric bud outgrowth by Pax2-dependent activation of the glial derived neurotrophic factor gene. *Development* **128**, 4747-4756.

Buttitta, L., Mo, R., Hui, C. C. and Fan, C. M. (2003). Interplays of Gli2 and Gli3 and their requirement in mediating Shh-dependent sclerotome induction. *Development* **130**, 6233-6243.

Cano-Gauci, D. F., Song, H. H., Yang, H., McKerlie, C., Choo, B., Shi, W., Pullano, R., Piscione, T. D., Grisaru, S., Soon, S. et al. (1999). Glypican-3-deficient mice exhibit the overgrowth and renal abnormalities typical of the Simpson-Golabi-Behmel syndrome. *J. Cell Biol.* **146**, 255-264.

Chen, J. K., Taipale, J., Cooper, M. K. and Beachy, P. A. (2002). Inhibition of Hedgehog signaling by direct binding of cyclopamine to Smoothened. *Genes Dev.* **16**, 2743-2748.

Chiang, C., Litingtung, Y., Lee, E., Young, K. E., Corden, J. L., Westphal, H. and Beachy, P. A. (1996). Cyclopia and defective axial patterning in mice lacking Sonic hedgehog gene function. *Nature* **383**, 407-413.

Conlon, R. A. and Herrmann, B. G. (1993). Detection of messenger RNA by in situ hybridization to postimplantation embryo whole mounts. *Methods Enzymol.* **225**, 373-383.

Dai, P., Akimaru, H., Tanaka, Y., Maekawa, T., Nakafuku, M. and Ishii, S. (1999). Sonic Hedgehog-induced activation of the Gli1 promoter is mediated by GLI3. *J. Biol. Chem.* **274**, 8143-8152.

Dressler, G. R., Deutsch, U., Chowdhury, K., Nornes, H. O. and Gruss, P. (1990). Pax-2, a new murine paired-box-containing gene and its expression in the developing excretory system. *Development* **109**, 787-795.

Grisaru, S., Cano-Gauci, D., Tee, J., Filmus, J. and Rosenblum, N. D. (2001). Glypican-3 modulates BMP- and FGF-Mediated Effects during Renal Branching Morphogenesis. *Dev. Biol.* **230**, 31-46.

Hu, M. C. and Rosenblum, N. D. (2005). Smad1, {beta}-catenin and Tcf4 associate in a molecular complex with the Myc promoter in dysplastic renal tissue and cooperate to control Myc transcription. *Development* **132**, 215-225.

Hu, M. C., Piscione, T. D. and Rosenblum, N. D. (2003). Elevated Smad1/b-catenin molecular complexes and renal medullary cystic dysplasia in ALK3 transgenic mice. *Development* **130**, 2753-2766.

Ikram, M. S., Neill, G. W., Regl, G., Eichberger, T., Frischauf, A. M., Aberger, F., Quinn, A. and Philpott, M. (2004). GLI2 is expressed in normal human epidermis and BCC and induces GLI1 expression by binding to its promoter. *J. Invest. Dermatol.* **122**, 1503-1509.

Ingham, P. W. and McMahon, A. P. (2001). Hedgehog signaling in animal development: paradigms and principles. *Genes Dev.* **15**, 3059-3087.

Kang, S., Graham, J. M., Jr, Olney, A. H. and Biesecker, L. G. (1997). GLI3 frameshift mutations cause autosomal dominant Pallister-Hall syndrome. *Nat. Genet.* **15**, 266-268.

Kim, P. C., Mo, R. and Hui, C. C. (2001). Murine models of VACTERL syndrome: Role of sonic hedgehog signaling pathway. *J. Pediatr. Surg.* **36**, 381-384.

Kinzler, K. W. and Vogelstein, B. (1990). The GLI gene encodes a nuclear protein which binds specific sequences in the human genome. *Mol. Cell. Biol.* **10**, 634-642.

Kohlhase, J., Wischermann, A., Reichenbach, H., Froster, U. and Engel, W. (1998). Mutations in the SALL1 putative transcription factor gene cause Townes-Brocks syndrome. *Nat. Genet.* **18**, 81-83.

Lai, K., Robertson, M. J. and Schaffer, D. V. (2004). The sonic hedgehog signaling system as a bistable genetic switch. *Biophys. J.* **86**, 2748-2757.

Li, Y., Zhang, H., Choi, S. C., Litingtung, Y. and Chiang, C. (2004). Sonic hedgehog signaling regulates Gli3 processing, mesenchymal proliferation, and differentiation during mouse lung organogenesis. *Dev. Biol.* **270**, 214-231.

Litingtung, Y. and Chiang, C. (2000). Specification of ventral neuron types is mediated by an antagonistic interaction between Shh and Gli3. *Nat. Neurosci.* **3**, 979-985.

Litingtung, Y., Dahn, R. D., Li, Y., Fallon, J. F. and Chiang, C. (2002). Shh and Gli3 are dispensable for limb skeleton formation but regulate digit number and identity. *Nature* **418**, 979-983.

Long, F., Zhang, X. M., Karp, S., Yang, Y. and McMahon, A. P. (2001). Genetic manipulation of hedgehog signaling in the endochondral skeleton reveals a

direct role in the regulation of chondrocyte proliferation. *Development* **128**, 5099-5108.
McDermott, A., Gustafsson, M., Elsam, T., Hui, C. C., Emerson, C. P., Jr and Borycki, A. G. (2005). Gli2 and Gli3 have redundant and context-dependent function in skeletal muscle formation. *Development* **132**, 345-357.
Methot, N. and Basler, K. (2001). An absolute requirement for Cubitus interruptus in Hedgehog signaling. *Development* **128**, 733-742.
Michael, L. and Davies, J. A. (2004). Pattern and regulation of cell proliferation during murine ureteric bud development. *J. Anat.* **204**, 241-255.
Mill, P., Mo, R., Hu, M. C., Dagnino, L., Rosenblum, N. D. and Hu, C.-C. (2005). Transcriptional and post-translational proliferative control by SHH-dependent GLI activator and repressor functions in the embryonic epidermis. *Developmental Cell* **9**, 293-303.
Mo, R., Freer, A. M., Zinyk, D. L., Crackower, M. A., Michaud, J., Heng, H. H., Chik, K. W., Shi, X. M., Tsui, L. C., Cheng, S. H. et al. (1997). Specific and redundant functions of Gli2 and Gli3 zinc finger genes in skeletal patterning and development. *Development* **124**, 113-123.
Moore, M. W., Klein, R. D., Farinas, I., Sauer, H., Armanini, M., Phillips, H., Reichardt, L. F., Ryan, A. M., Carver-Moore, K. and Rosenthal, A. (1996). Renal and neuronal abnormalities in mice lacking GDNF. *Nature* **382**, 76-79.
Nishinakamura, R., Matsumoto, Y., Nakao, K., Nakamura, K., Sato, A., Copeland, N. G., Gilbert, D. J., Jenkins, N. A., Scully, S., Lacey, D. L. et al. (2001). Murine homolog of SALL1 is essential for ureteric bud invasion in kidney development. *Development* **128**, 3105-3115.
Park, H. L., Bai, C., Platt, K. A., Matise, M. P., Beeghly, A., Hui, C. C., Nakashima, M. and Joyner, A. L. (2000). Mouse Gli1 mutants are viable but have defects in SHH signaling in combination with a Gli2 mutation. *Development* **127**, 1593-1605.
Pichel, J. G., Shen, L., Sheng, H. Z., Granholm, A.-C., Drago, J., Grinberg, A., Lee, E. J., Huang, S. P., Saarmas, M., Hoffer, B. J. et al. (1996). Defects in enteric innervation and kidney development in mice lacking GDNF. *Nature* **382**, 73-76.
Piscione, T. D. and Rosenblum, N. D. (1999). The malformed kidney: disruption of glomerular and tubular development. *Clin. Genet.* **56**, 343-358.
Piscione, T. D., Yager, T. D., Gupta, I. R., Grinfeld, B., Pei, Y., Attisano, L., Wrana, J. L. and Rosenblum, N. D. (1997). BMP-2 and OP-1 exert direct and opposite effects on renal branching morphogenesis. *Am. J. Physiol.* **273**, F961-F975.
Rallu, M., Machold, R., Gaiano, N., Corbin, J. G., McMahon, A. P. and Fishell, G. (2002). Dorsoventral patterning is established in the telencephalon of mutants lacking both Gli3 and Hedgehog signaling. *Development* **129**, 4963-4974.
Rothenpieler, U. W. and Dressler, G. R. (1993). Pax-2 is required for mesenchyme-to-epithelium conversion during kidney development. *Development* **119**, 711-720.
Sanyanusin, P., Schimmenti, L. A., McNoe, L. A., Ward, T. A., Pierpont, M. E. M., Sullivan, M. J., Dobyns, W. B. and Eccles, M. R. (1995). Mutation of the *PAX2* gene in a family with optic nerve colobomas, renal anomalies and vesicoureteral reflux. *Nat. Genet.* **9**, 358-363.
Sasaki, H., Hui, C., Nakafuku, M. and Kondoh, H. (1997). A binding site for Gli proteins is essential for HNF-3beta floor plate enhancer activity in transgenics and can respond to Shh in vitro. *Development* **124**, 1313-1322.
Schimmang, T., Lemaistre, M., Vortkamp, A. and Ruther, U. (1992). Expression of the zinc finger gene Gli3 is affected in the morphogenetic mouse mutant extra-toes (Xt). *Development* **116**, 799-804.
Stoykova, A. and Gruss, P. (1994). Roles of Pax-genes in developing and adult brain as suggested by expression patterns. *J. Neurosci.* **14**, 1395-1412.
Torres, M., Gomez-Pardo, E., Dressler, G. R. and Gruss, P. (1995). *Pax-2* controls multiple steps of urogenital development. *Development* **121**, 4057-4065.
Wang, B., Fallon, J. F. and Beachy, P. A. (2000). Hedgehog-regulated processing of Gli3 produces an anterior/posterior repressor gradient in the developing vertebrate limb. *Cell* **100**, 423-434.
Yu, J., Carroll, T. J. and McMahon, A. P. (2002). Sonic hedgehog regulates proliferation and differentiation of mesenchymal cells in the mouse metanephric kidney. *Development* **129**, 5301-5312.
Zhang, S. L., Moini, B. and Ingelfinger, J. R. (2004). Angiotensin II increases Pax-2 expression in fetal kidney cells via the AT(2) receptor. *J. Am. Soc. Nephrol.* **15**, 1452-1465.